

Improving TDS Sensor Accuracy in an IoT-Based Fertigation Prototype Using Polynomial Regression Calibration and Interpolation

Arif Harjanto^{1*}, Happy Nugroho¹, Aprilia Amrina Ainurrosyidah¹, Aji Ery Burhandenny²

¹Department of Electrical Engineering, Faculty of Engineering, Mulawarman University, Indonesia

²Department of Electrical Engineering, Faculty of Engineering, Yogyakarta University, Indonesia

*Corresponding author Email: arif.harjanto@unmul.ac.id

The manuscript was received on 22 July 2025, revised on 28 August 2025, and accepted on 28 December 2025, date of publication 20 January 2026

Abstract

Accurate measurement of Total Dissolved Solids (TDS) is a critical requirement for hydroponic nutrient management, especially in automated fertigation systems that adjust nutrient concentrations based on plant age. However, non-industrial TDS sensors often exhibit significant fluctuations and non-linear errors, leading to unreliable nutrient dosing. This study proposes a calibration approach using second-order polynomial regression combined with interpolation to improve the accuracy of TDS measurements in an IoT-based fertigation prototype for lettuce hydroponics. The calibration was performed using reference TDS solutions and a digital TDS meter to ensure accurate measurements. The results show that the Mean Absolute Percentage Error (MAPE) decreased from 24.771% to 7.5768% during calibration, demonstrating a significant improvement in measurement accuracy. The calibrated sensor readings fall within the acceptable range for hydroponic nutrient control ($\pm 10\%$). This method provides a low-cost, reliable alternative for improving sensor accuracy in IoT fertigation systems.

Keywords: ESP32, Fertigation, IoT, Polynomial Regression, TDS Sensor Calibration.

1. Introduction

Smart farming technologies have been increasingly adopted to address agricultural challenges such as land scarcity, labour efficiency, and precision nutrient management. Hydroponic systems, particularly the Nutrient Film Technique (NFT), require precise monitoring of nutrient concentrations to maintain optimal Total Dissolved Solids (TDS) levels at each plant growth stage. Lettuce typically requires a nutrient concentration of approximately 300-900 ppm, with the specific level depending on the plant's age [1]–[4]. Previous studies indicate that automation and calibration techniques are crucial for improving the accuracy and stability of nutrient monitoring systems. [5] reported that applying linear regression calibration significantly improved TDS sensor accuracy, particularly when using microcontrollers with stable ADC performance. However, this approach alone is insufficient to address noise and nonlinearity commonly found in low-cost TDS sensors.

Subsequent studies demonstrated that combining regression-based calibration with signal filtering techniques can further enhance measurement reliability. Polynomial regression methods, such as the sectioned polynomial regression proposed by [6], effectively reduced MAE and RMSE values and expanded the operational range of low-cost TDS sensors. Similarly, [7] showed that polynomial correction combined with moving-average filtering significantly reduced measurement errors in DFRobot TDS sensors.

Furthermore, Kalman and moving-average filtering techniques have been proven effective for suppressing noise and stabilising TDS sensor data in IoT-based monitoring systems [8]–[10]. These findings suggest that hybrid calibration approaches integrating filtering and regression are highly suitable for improving TDS sensor accuracy, as reflected by reductions in MAPE, MAE, and RMSE, particularly in hydroponic applications.

Non-industrial analogue TDS sensors are widely used in IoT systems due to their affordability, but they suffer from nonlinearity, electrical noise, and temperature sensitivity, resulting in large errors (20-45%). These errors directly affect nutrient mixing accuracy, thereby reducing crop performance. Most existing studies focus on system automation and monitoring, but do not address the core problem of measurement error from the TDS sensor itself, which becomes critical when the system controls nutrient dosing automatically. This study focuses on improving TDS sensor accuracy during calibration using mathematical methods, such as polynomial regression and interpolation. The calibration model is embedded into an ESP32-based IoT fertigation prototype integrated with Thingier.io for real-time monitoring. Polynomial curve fitting is applied to correct the non-linear sensor response and stabilise signal fluctuations within the system.

Based on the explanation above, the goal is to develop a reliable, low-cost method to improve TDS sensor measurement accuracy for automated hydroponic nutrient control.



2. Literature Review

2.1. AB-Mix Nutrient Concentration for Lettuce

The growth process of lettuce begins with seed germination, in which lettuce seeds are sown into pre-moistened rockwool. The seedlings are maintained for approximately 10 DAS (days after sowing) or until they develop three to four leaves, after which they are transferred to a hydroponic installation for the growth and harvesting phase. The nutrient concentrations for hydroponically grown lettuce vary across different references and cultivation practices [11]. According to [11], the required nutrient concentration for lettuce after transplanting to the hydroponic system ranges from 300 to 500 ppm. The study by [12] reported that lettuce aged 2 to 13 DAP (days after transplanting) should receive 425 ppm, 14 to 23 DAP should receive 570 ppm, 24 to 30 DAT should receive 745 ppm, and 31 to 35 DAP should receive 800 ppm. Furthermore, [13] suggested that during the germination phase (weeks 1–3), the nutrient solution should have an electrical conductivity (EC) of 0.8-1.2 mS/cm, equivalent to approximately 400-600 ppm (Maylissa, 2015). During the vegetative-to-harvest phase (weeks 4–5), the recommended EC value ranges from 1.2 to 1.8 mS/cm, or approximately 600 to 900 ppm (Maylissa, 2015). Supporting this, [14] compared lettuce growth at various nutrient concentrations and found that 900 ppm resulted in better growth and yield during the third and fourth weeks of cultivation.

2.2. Polynomial Regression

Polynomial regression is a type of multiple linear regression formed by adding the influence of a predictor variable (X) raised to increasing powers up to the n-th order [15]. The general form of the polynomial regression equation is shown in Equation (1), while the error value equations are presented in Equations (2)–(4).

$$y = a_0 + a_1x + a_2x^2 + a_3x^3 + \dots + a_nx^n \dots\dots\dots (1)$$

$$Dt^2 = \sum_{i=1}^n (y_i - \bar{y})^2 \dots\dots\dots (2)$$

$$D^2 = \sum_{i=1}^n (y_i - a_0 - a_1x - a_2x^2 - a_3x^3 - \dots - a_nx^n)^2 \dots\dots\dots (3)$$

$$r = \sqrt{\frac{Dt^2 - D^2}{Dt^2}} \dots\dots\dots (4)$$

In this study, a second-order polynomial regression model was used, which can be represented as follows:

$$y = a_0 + a_1x + a_2x^2 \dots\dots\dots (5)$$

where:

y= response variable

x= predictor variable

a_nx^n = unknown parameter of the n-th order

D_t = total data variation (relative to the mean)

D= unexplained variation (error)

r= correlation coefficient

To determine the coefficients a_0 , a_1 , and a_2 The following system of equations is used:

$$\begin{bmatrix} n & \sum x & \sum x^2 \\ \sum x & \sum x^2 & \sum x^3 \\ \sum x^2 & \sum x^3 & \sum x^4 \end{bmatrix} \begin{bmatrix} a_0 \\ a_1 \\ a_2 \end{bmatrix} = \begin{bmatrix} \sum y \\ \sum xy \\ \sum x^2y \end{bmatrix} \dots\dots\dots (6)$$

Equation (6) can be solved using methods such as Gaussian elimination, Gauss–Jordan elimination, iteration, and other numerical approaches [16]–[18].

2.3. Mean Absolute Percentage Error (MAPE)

Mean Absolute Percentage Error (MAPE) is used to evaluate the accuracy of prediction models by measuring the average absolute deviation between the predicted and actual values, expressed as a percentage of the actual value, using the formula:

$$MAPE = \frac{1}{n} \sum \left| \frac{Actual - Predicted}{Actual} \right| \times 100\% \dots\dots\dots (7)$$

A lower MAPE indicates better model accuracy, while higher values suggest poorer performance [19]. According to [20], model accuracy can be classified based on MAPE values : less than 10% indicates *very high accuracy*, 10 to 20% indicates *good accuracy*, 20 to 50% indicates *reasonable accuracy*, and more than 50% indicates *poor accuracy*.

3. Method

3.1. Overall System Design

The block diagram of the fertigation and nutrient refill system is shown in Fig.1, illustrating the integration of the components used in this study.



Fig 1. Block Diagram

In the input section, the electrical energy for all components is provided by the power supply, including the HC-SR04 ultrasonic sensor, TDS sensor, and RTC module. In the input section, the electrical energy for all components is provided by the power supply, including the HC-SR04 ultrasonic sensor, TDS sensor, and RTC module. The NodeMCU ESP32 microcontroller processes the data acquired from the sensors and the RTC module. Afterwards, the NodeMCU ESP32 transmits the processed data to a relay, activating or deactivating the pumps based on predefined conditions. The flowchart of the nutrient mixing and refilling process is shown in Fig.4.

Additionally, the sensor readings are stored on a microSD card through the SD module as backup in case they are not recorded in the Thingier.io data buckets. Thingier.io stores data in its data buckets, displays sensor readings on the dashboard, and sends email notifications when certain conditions are triggered.

The schematic circuit for the TDS sensor used in this study is shown in Fig. 2, which illustrates the wiring configuration and signal connections between the TDS module and the ESP32 microcontroller.

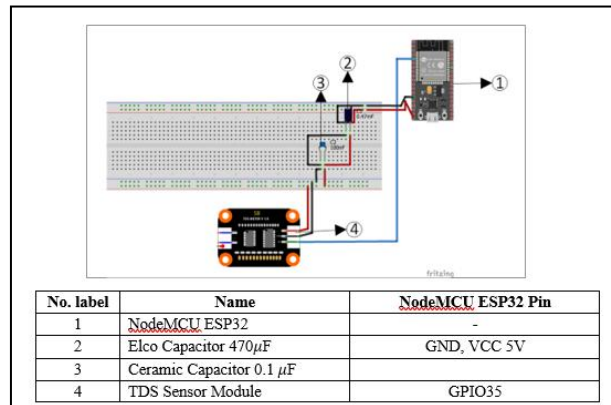


Fig 2. Schematic Diagram Circuit for the TDS sensor

The design of the fertigation and nutrient refill system prototype is shown in Figure 3.

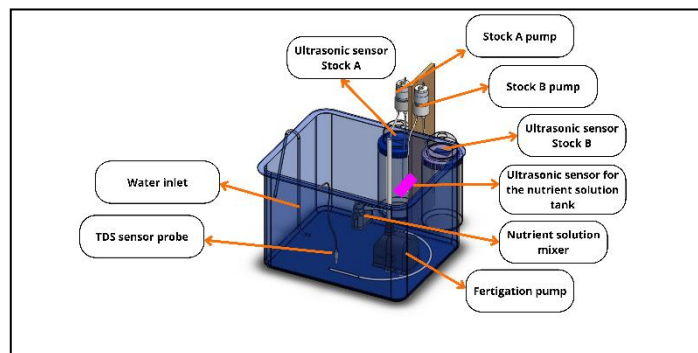


Fig 3. Prototype System Design of the Proposed Work

3.2. System Works

As the TDS sensor's accuracy is the primary focus of this study, methodological emphasis is placed on calibration rather than the overall fertigation workflow. Therefore, the calibration procedure is summarised in the flowchart shown in Fig. 4, which outlines the key steps of data collection, polynomial regression modelling, interpolation, and error evaluation used to develop the calibration model applied in this research.

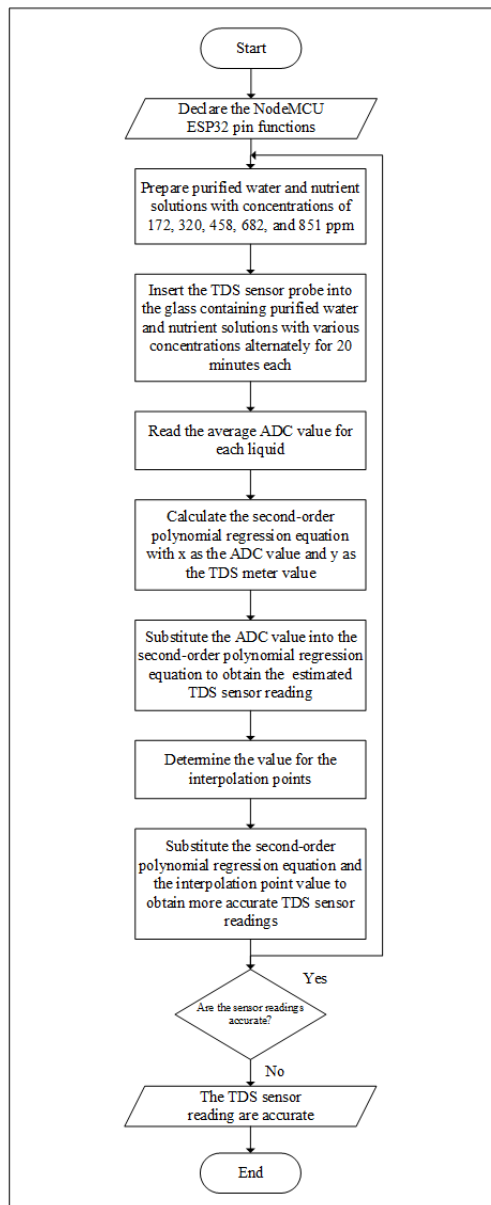


Fig 4. TDS Sensor Calibration Flowchart

3.3. Test Method

This study focuses on improving the calibration and accuracy of the TDS sensor; therefore, the testing procedure evaluated the sensor's performance before and after calibration. The experimental tests were conducted specifically on the TDS sensing subsystem rather than on the full fertigation workflow.

The calibration test involved collecting raw TDS sensor readings from several known reference solutions, with a digital TDS meter serving as the ground truth. These collected data were used to develop the polynomial regression model and the interpolation process. After generating the calibration equation, a second round of testing was performed using reference concentrations that closely approximated the initial calibration values to validate the improvement in accuracy.

This calibration-focused testing approach ensured that the resulting regression model was reliable before being integrated into the full IoT fertigation system. Thus, the primary objective of the test method was to quantify error reduction through MAPE analysis and confirm the effectiveness of the proposed calibration technique.

4. Results and Discussion

4.1 Calibration Process

This calibration-focused testing approach ensured that the resulting regression model was reliable before being integrated into the full IoT fertigation system. Thus, the primary objective of the test method was to quantify error reduction through MAPE analysis and confirm the effectiveness of the proposed calibration technique.

The calibration process was carried out using several concentrations of AB-mix nutrient solution, with each concentration measured using a digital TDS meter as the reference value. A second-order polynomial regression model was constructed using the corresponding raw ADC readings obtained from the TDS sensor. The non-linear relationship between the sensor's ADC values and the actual TDS meter concentration is represented by this regression equation.

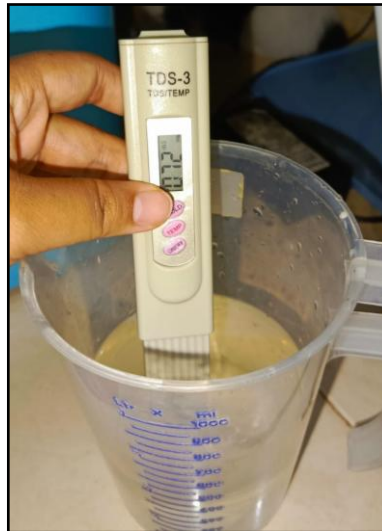


Fig 5. Measurement of Solution Concentration

Using the resulting polynomial Equation, estimated TDS values were calculated for each ADC reading, thereby determining the calibration points needed for the interpolation. Table 1 shows the dataset obtained before calibration, showing the discrepancy between the reference TDS meter readings and the uncalibrated sensor output. The complete calibration dataset consists of 65 data points; however, only 30 representative data points are shown in Table 1 for clarity and to avoid redundancy in the manuscript.

Table 1. Dataset Obtained Before Calibration

Mean ADC Value	TDS Meter	TDS sensor	Percentage Error (%)
93,2	80	105,55	31,938
94,9	80	105,85	32,313
96,1	80	106	32,500
93,8	80	105,09	31,363
94,3	80	105,03	31,288
320,5	172	95,93	44,227
317,1	172	95,79	44,308
328,1	172	95,83	44,285
327,9	172	95,8	44,302
331,4	172	95,87	44,262
Mean ADC Value	TDS Meter	TDS sensor	Percentage Error (%)
594	320	204,36	36,138
617,4	320	220,44	31,113
611,3	320	216,27	32,416
613,8	320	217,97	31,884
592,8	320	204,01	36,247
789,7	458	356,99	22,055
801,1	458	358	21,834
795,5	458	358,42	21,742
789,5	458	358,92	21,633
800,1	458	362,04	20,952
961,7	682	560,85	17,764
947,9	682	556,61	18,386
929,6	682	550,39	19,298
958,8	682	551,79	19,092
987,8	682	552,92	18,927
1107,9	851	708,25	16,774
1102,1	851	718,86	15,528
1183,4	851	725,31	14,770
1183,4	851	731,83	14,004
1099,5	851	739,48	13,105
MAPE			24,771 %

From the ADC values obtained during testing, a scatter plot and the corresponding second-order polynomial regression curve were generated to model the sensor's behaviour. The polynomial graph and its regression equation are shown in Fig. 6, which illustrates the sensor's non-linear response across the tested concentration range.

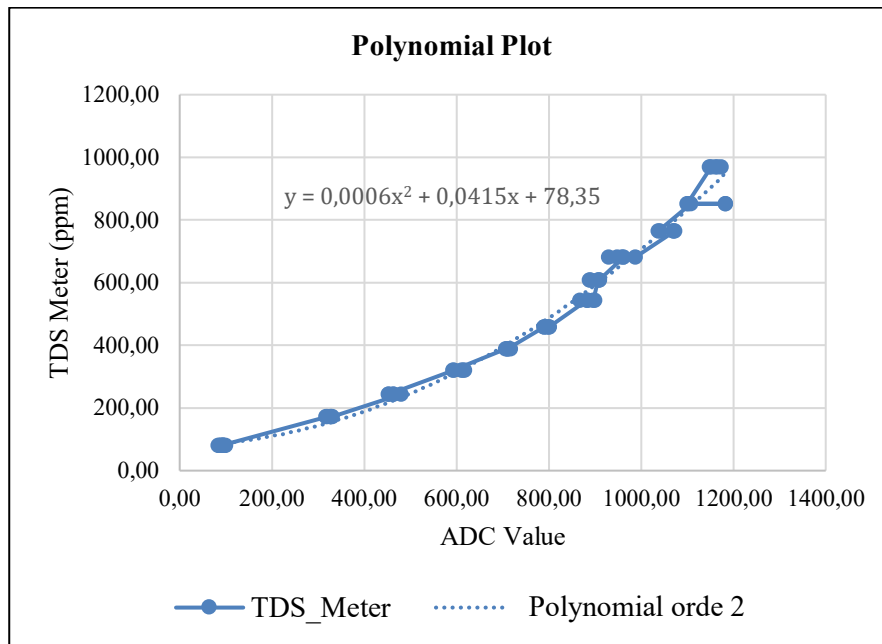


Fig 6. Polynomial Plot

Based on the regression equation shown in Fig. 6, several calibration points were determined and subsequently used as reference intervals for interpolation. This process produced a refined set of corrected sensor readings. The results of calibrated TDS sensor values are shown in Table 2, demonstrating the accuracy improvement achieved through polynomial regression and interpolation.

Table 2. Dataset Obtained After Calibration

TDS Meter	TDS sensor	Percentage Error (%)
72	46,53	35,375
72	59,92	16,778
72	73,9	2,639
72	87,81	21,958
72	95,11	32,097
168	151,55	9,792
168	156,53	6,827
TDS Meter	TDS sensor	Percentage Error (%)
168	169,13	0,673
168	181,33	7,935
168	192,75	14,732
315	297,94	5,416
315	307,67	2,327
315	317,15	0,683
315	323,66	2,749
315	329,8	4,698
492	435,54	11,476
492	467,49	4,982
492	503,51	2,339
492	535,51	8,843
492	564,23	14,681
630	636,91	1,097
630	635,06	0,803
630	635,07	0,805
630	667,72	5,987
630	666,01	5,716
811	796,23	1,821
811	804,04	0,858
811	815,08	0,503
811	818,85	0,968
811	823,1	1,492
MAPE		7,568 %

4.2. Improvement Analysis

The Mean Absolute Percentage Error (MAPE) values obtained before and after calibration are presented in Tables 1 and 2, respectively. Before calibration, the TDS sensor exhibited a relatively high MAPE value of **24.771%**, indicating a substantial discrepancy between the sensor measurements and the reference TDS meter readings. This result demonstrates that the uncalibrated sensor's raw output lacks sufficient accuracy and is affected by systematic measurement errors across the tested concentration range.

After calibration using a polynomial regression equation, a significant quantitative improvement in measurement accuracy was observed. The MAPE value decreased to **7.568%**, reflecting a reduction in error of more than **70%** compared to the initial uncalibrated condition. This considerable decrease indicates that the calibration process effectively minimised the deviation between the sensor readings and the reference measurements.

The numerical comparison of error values before and after calibration clearly shows that the calibrated sensor produces measurements that are substantially closer to the reference TDS meter. These results provide objective evidence that the applied calibration method enhances the overall accuracy of the TDS sensor. Therefore, from a quantitative performance perspective, the calibration process effectively improves the reliability of the sensor output for subsequent measurement and analysis.

4.3. Discussion

The observed improvement in measurement accuracy can be attributed to the application of polynomial regression, which effectively addresses the TDS sensor's inherent nonlinearity. Unlike linear calibration approaches, polynomial regression allows the calibration curve to better represent complex sensor response characteristics across the entire measurement range. As a result, systematic deviations between the raw sensor output and the reference values can be corrected more effectively, leading to more consistent sensor behaviour.

In addition to regression-based calibration, the use of interpolation techniques to stabilise the Analog-to-Digital Converter (ADC) input further improved overall accuracy. By processing multiple sensor readings and computing a representative value, interpolation reduced the influence of short-term fluctuations caused by electrical noise, water movement, and pump activation. This stabilisation process enabled the microcontroller to obtain smoother, more reliable TDS measurements during continuous operation.

Another important finding is that the calibrated sensor demonstrated stable performance when evaluated using a validation dataset with reference concentrations that differed slightly from those used during calibration (e.g., 80→72 ppm, 172→168 ppm). This behaviour indicates that the regression model does not merely memorise specific calibration points but can generalise across neighbouring concentration ranges. Such generalisation is essential for practical applications, where nutrient concentrations may vary dynamically over time.

Overall, the calibrated TDS sensor consistently produced readings within **10%** of the reference measurements. This level of accuracy falls within an acceptable tolerance range for hydroponic nutrient management systems. Maintaining nutrient concentration within this range is critical for ensuring optimal plant growth, nutrient uptake efficiency, and overall crop productivity. Consequently, the proposed calibration and signal-stabilisation approach demonstrates strong potential for reliable, real-time nutrient monitoring in hydroponic applications.

5. Conclusion

This study demonstrates that the measurement accuracy of a non-industrial analogue TDS sensor can be significantly enhanced through the application of calibration techniques based on mathematical modelling, specifically polynomial regression and interpolation. The calibration process effectively corrects the sensor's inherent nonlinearity, which is commonly found in low-cost analogue sensing devices. As a result, systematic deviations between the raw sensor output and the reference TDS meter measurements can be substantially reduced. Quantitative evaluation using the Mean Absolute Percentage Error (MAPE) metric shows that the proposed calibration approach successfully reduced the error from **24.771%** in the uncalibrated condition to **7.568%** after calibration. This corresponds to an overall accuracy improvement of approximately **72.5%**, clearly indicating the effectiveness of the implemented method. Such a significant reduction in error confirms that the calibrated sensor can provide more consistent and reliable measurements across the tested nutrient concentration range.

Furthermore, integrating the calibrated TDS sensor into an Internet of Things (IoT)-based fertigation system enhances the reliability of real-time nutrient monitoring and control. Accurate and stable TDS measurements enable more precise nutrient dosing, which is essential for maintaining optimal nutrient concentrations in hydroponic systems. Consequently, the proposed approach supports the implementation of precision hydroponics by improving nutrient management efficiency, reducing the risk of over- or under-fertilisation, and enhancing plant growth and overall system performance.

References

- [1] A. Firmansah and Aripriharta, *Panduan Praktis Smart Aquaponik*. Palembang: Jakarta: Bening Media Publishing, 2021.
- [2] N. Aini and N. Azizah, *Teknologi Budidaya Tanaman Sayuran secara Hidroponik*. Malang: Malang: UB Press, 2018. [Online]. Available: https://www.google.co.id/books/edition/Teknologi_Budidaya_Tanaman_Sayuran_secar/IMuEDwAAQBAJ?hl=id&gbpv=0
- [3] K. Herwibowo and N. S. Budiana, *Hidroponik Sayuran, IV*. Jakarta: Jakarta: Penebar Swadaya Grup, 2016. [Online]. Available: <https://books.google.co.id/books?id=ttoQBwAAQBAJ>
- [4] Y. Harsono, *Sukses Hidroponik Untuk Pemula*. Semarang: Semarang: Laksana, 2020. [Online]. Available: <https://books.google.co.id/books?id=fQjZzwEACAAJ>
- [5] D. R. Tisna, B. Juliartha, M. Putra, and T. Maharani, "Metode Peningkatan Akurasi pada Sensor TDS Berbasis Arduino untuk Nutrisi Air Menggunakan Regresi Linier," vol. 14, no. 1, pp. 61–68, 2022.
- [6] A. Jamil, T. S. Ting, Z. Z. Abidin, and M. Othman, "Polynomial Regression Calibration Method of Total Dissolved Solids Sensor for Hydroponic Systems," vol. 31, no. 6, pp. 2769–2782, 2023.
- [7] I. Georgantas, S. Mitropoulos, S. Katsoulis, and I. Chronis, "Integrated Low-Cost Water Quality Monitoring System Based on LoRa Network," pp. 1–17, 2025.
- [8] A. Y. Yaakob, M. H. Azham, and M. H. M. Ramli, "Kalman Filter-Based Data Stabilization for an Automated Water Quality

- Monitoring System in *Macrobrachium Rosenbergii* Larvae Culture,” pp. 157–176, 2024.
- [9] M. Misbahuddin, N. Cokrowati, A. Amrullah, and L. Ernawati, “Kalman Filter-Enhanced Data Aggregation in LoRaWAN-Based IoT Framework for Aquaculture Monitoring in,” pp. 1–23, 2025.
- [10] A. Ma, A. Anggari, and R. Ikhsan, “Kalman Filter for Noise Reducer on Sensor Readings,” vol. 1, no. 2, pp. 10–21, 2019.
- [11] N. Zahra, C. Muthiadin, and F. Ferial, “Budidaya tanaman selada (*Lactuca sativa* L.) secara hidroponik dengan sistem DFT di BBPP Batangkaluku,” *Filogeni J. Mhs. Biol.*, vol. 3, no. 1, pp. 18–22, 2023, doi: 10.24252/filogeni.v3i1.29922.
- [12] F. Sulaiman et al., “Budidaya Selada Secara Hidroponik di Balai Pengkajian Teknologi Pertanian Jalan Mentok, Kepulauan Bangka Belitung,” *Pros. Semin. Nas. Lahan Suboptimal ke-11*, vol. 6051, pp. 230–236, 2023.
- [13] K. Vought et al., “Dynamics of micro and macronutrients in a hydroponic nutrient film technique system under lettuce cultivation,” *Heliyon*, vol. 10, no. 11, p. e32316, 2024, doi: 10.1016/j.heliyon.2024.e32316.
- [14] M. Asrori and M. H. Murdani, “Sistem Pemberian Nutrisi Pada Tanaman Hidroponik Menggunakan Metode Fuzzy Berbasis Arduino,” *J. Syst. Eng. Technol. Innov.*, vol. 2, no. 01, pp. 91–99, 2023, doi: 10.38156/jisti.v2i01.37.
- [15] R. Sarno, S. I. Sabilla, Malikhah, D. P. Purbawa, and M. S. H. Ardani, *Machine Learning dan Deep Learning-Konsep dan Pemrograman Python*. Penerbit Andi, 2022. [Online]. Available: <https://books.google.co.id/books?id=byWFEAAAQBAJ>
- [16] I. K. A. Atmika, “Diktat Mata Kuliah Metode Numerik,” Univ. Udayana, pp. 50–57, 2016, [Online]. Available: https://kupdf.net/download/metode-analisa-numerik-rinaldi-munir_58fabb1cdc0d60af0b959e85_pdf#
- [17] Stephen B. Vardeman and J. Marcus Jobe, *Basic Engineering And Data Collection Analysis*. United States: Iowa State University Digital Press, 2023.
- [18] J. Walrand, *Probability in Electrical Engineering and Computer Science*. Berkeley: University of California, 2022.
- [19] R. A. Yaffee and M. McGee, *An Introduction to Time Series Analysis and Forecasting: With Applications of SAS® and SPSS®*. Amsterdam: Amsterdam: Academic Press, 2000. [Online]. Available: <https://books.google.co.id/books?id=LSojZBiBZBgC>
- [20] I. Nabillah and I. Ranggadara, “Mean Absolute Percentage Error untuk Evaluasi Hasil Prediksi Komoditas Laut,” *JOINS (Journal Inf. Syst.*, vol. 5, no. 2, pp. 250–255, 2020, doi: 10.33633/joins.v5i2.3900.